IOP Publishing

Analytical Techniques for Biomedical Nanotechnology

Ajeet Kaushik, Sesha S Srinivasan and Yogendra Kumar Mishra

Chapter 15

Microfluidics system for biomedical nanotechnology

Nitish Sagar, Prosenjit Sen and Saurabh Kumar

This chapter presents an overview of microfluidic systems from a biomedical perspective. The physics of microscale fluid flow and fabrication methods of microfluidic chips are discussed in the first section. Later, we highlight the major applications of such microfluidic devices in biomedical areas of research. The use of microfluidic devices in single-cell analysis, polymerase chain reaction (PCR) study, biosensors integration, and organ-on-chip technology is explained in detail. We understand the vastness of this area and thus it is not possible to cover all aspects of the microfluidic systems in a single chapter. However, this chapter will provide general knowledge to help readers become acquainted with such microfluidic systems used in biomedical research.

15.1 Introduction

The principle of miniaturization of devices that once started in the microelectronics industry has reached the domain of fluid mechanics. With the technological advancements in nano-fabrication techniques, researchers have discussed the many benefits of miniaturization that enhance device performance, reduce power consumption, and integrate several functionalities within a small area. This miniaturization concept has been a boon to fluid research and has given rise to a new area, i.e., *microfluidics*. Microfluidics refers to the science of manipulating fluid volumes in the range of micro- to femto-litres with the help of tens to hundreds of micrometers dimension of channels. The reduction in channel size increases the surface-to-volume ratio, and interestingly, surface forces become dominant. These forces play a significant role in the study of microfluidics. Usually, fluid flow is turbulent in nature; however, in the microfluidics channel, the nature of fluid flow is laminar. This is because viscous forces are predominant over inertial forces.

doi:10.1088/978-0-7503-3379-5ch15

It is important to know how this microscale flow science turned into a technological advancement for several research areas. The area of microfluidics developed from different research domains that require precise fluid flow control. As we know, microanalytical techniques like gas-phase chromatography, high-pressure liquid chromatography, and capillary electrophoresis significantly improved chemical analysis. This quest for compact and microscale methods, led to microfluidic device research. The second development came as part of Defense Advanced Research Projects Agency (DARPA) research programs after the end of the Cold War in the 1990s, aimed at developing a portable device to detect chemical and biological threats. This enhanced academic research in microfluidics. The genomics studies, such as DNA sequencing and other micro-analysis related to molecular biology, gave another boost to microfluidics. It offered high throughput and better sensitivity than that of conventional methods. Another contribution was from the field of microelectronics. The silicon-based and micro-electromechanical systems (MEMS) fabrication techniques such as photolithography were used to develop microfluidic devices. Although later, most microfluidic chip researchers opted for an elastomer like polydimethylsiloxane (PDMS), for its inexpensive, optical transparency and biocompatible nature.

Microfluidics offers several advantages: low sample volume consumption, high throughput, low risk of contamination, parallelization of multiple assays, and the ability to integrate multiple detection techniques with microfluidic devices for real-time testing, thus making it an ideal candidate for point-of-care (POC) and lab-on-chip devices. As mentioned above, the benefits of a microfluidic platform stimulated many biological research areas like single-cell study, point-of-care devices for rapid testing, biosensors, mimicking body physiology on chips to study cancer and its metastasis (organ-on-chip), etc.

In this chapter, we will discuss the physics of micro-scale flows explaining the fluid mechanics and how it is different from the bulk flow. The next section will cover various aspects of device fabrication, such as soft lithography, micromachining, and 3D printing. In the last sections, we will cover several applications of microfluidic platforms such as single-cell analysis, PCR-based study, biosensors integration, and organ-on-chip research.

15.2 Physics of micro-scale fluid flow

Microfluidics deals with fluid phenomena that are quite like bulk fluid mechanics, but the surface forces at the microscale are dominant. Unlike in macroscale flows, fluid is not in turbulent flow regime. But in the microfluidics purview, surface tension and surface engineering play an important role in several applications. There are two types of approach in microchannel-based fluid flow—continuous microfluidics and droplet microfluidics [1]. There is another area of research, popularly known as digital microfluidics [2] (manipulation of discrete droplets on planar patterned substrate). For this, different types of forces such as surface acoustic wave (SAW) [3], magnetic force [4], thermocapillary, optical force, electrical force [5], or a combination are used to carry out droplet manipulation.

This section will start with the general conservation equations (mass and momentum) using the Reynolds transport theorem to explain fluid flow mechanics in microchannels, followed by wettability and surface tension. In the later part, we briefly discuss important non-dimensional numbers and its practical relevance in continuous and droplet microfluidics areas. It is to be noted that several conventional fluid mechanics concepts hold true for microfluidic study, and thus we do not include those in this section.

15.2.1 Reynolds transport theorem and conservation equations

Let us take an example to explain general conservation law. Consider an imaginary box of money in which you stored an amount (this we call 'In'). Later, you take out some of the stored money (this we call 'Out'). Also, consider some interest you get for keeping money in the box (this is 'Generation'). You would like to know the net change in your deposit (this is 'Change'). The general intuitive maths suggests:

$$\textbf{In} - \textbf{Out} + \textbf{Gen} = \textbf{Change}$$

$$\text{Or } \textbf{rate of (In} - \textbf{Out} + \textbf{Gen)} = \textbf{rate of (change)}$$

We introduce the 'rate of' to calculate the amount with respect to time. This equation of conservation, from the first principle that we get from simple mathematics, also holds for our conservation equations for mass, momentum, or energy.

However, there is another way to discuss these conservation equations in fluid flow, which is known as the Reynold transport theorem (RTT). This theorem bridges the gap between the Lagrangian and Eulerian approach to fluid mechanics. In the Lagrangian method, fluid flow is described by tracing individual fluid particles, while in the Eulerian method, fluid is described using the control volume approach. As we know that our classical physics laws are defined for a system approach, it is essential to have mathematical modeling of those in the control volume approach to study fluid flow either in differential or integral form.

The Reynolds transport theorem relates the control mass system and control volume approach. The general expression of RTT is given by:

$$\left(\frac{dN}{dt}\right)_{\text{sys}} = \frac{\partial}{\partial t}\iiint \rho n d \forall + \iint n\rho \vec{V} \cdot dA \tag{15.1}$$

where N is any extensive fluid property, n is the intensive fluid property that is N per unit mass, ρ is the fluid density, $d\forall$ represents elementary volume, and dA represents an elementary area of the control surface. $\vec{V}$ is the velocity property crossing the control surface. The left-hand side represents the rate of property change in the system, while the right-hand side of the equation tells us about its net effect in the control volume method. The first term on the right-hand side represents the rate of change of fluid property in control volume, and the second term gives the rate of (outflow–inflow) of the property from the control surface.

This RTT can get conservation equations of mass and momentum by substituting the '*N*' value in equation (15.1). In the mass conservation equation, *N* is mass '*M*' and thus *n* is '1'. Since the mass of the system is conserved, thus the rate of change of mass of the system, *dM*/*dt* is zero that leads to a mass conservation equation as:

$$\frac{\partial}{\partial t}\iiint \rho d\forall + \iint \rho \vec{V} \cdot dA = 0 \tag{15.2}$$

Since the elementary volume choice is arbitrary, the derivative term can be placed within an integral operator in the first term in equation (15.2). Using the Gauss divergence theorem to convert the area integral into volume integral in the second term, we get:

$$\frac{\partial \rho}{\partial t} + \nabla \cdot \left(\rho \vec{V}\right) = 0 \tag{15.3}$$

Equation (15.3) represents the mass conservation equation in differential form.

Let us take an example to elucidate this concept. Consider one-dimension steady flow (velocity and other fluid properties at any location do not change with time) through a variable area channel (figure 15.1).

The corresponding continuity equation is $\nabla \cdot (\rho \vec{V}) = 0$. Integrating it over an elemental volume $d\forall$ and using divergence theorem, we get $\iint (\rho \vec{V}) \cdot \hat{n} dA = 0$ where $\hat{n}$ is a unit normal vector to dA. Since the velocity is zero at all boundaries except at inlet and outlet, the above expression can be written as:

$$\left(\iint (\vec{\mathbf{V}}\rho) \cdot \hat{\boldsymbol{n}}\,\mathbf{dA}\right)_{\mathbf{in}} + \left(\iint (\vec{\mathbf{V}}\rho) \times \hat{\boldsymbol{n}}\,\mathbf{dA}\right)_{\mathbf{tuo}} = 0 \tag{15.4}$$

At inlet, $\hat{n}$ is $-\hat{i}$ and at outlet $\hat{n}$ is $\hat{i}$. With u as x-component of velocity, we can write:

$$-\left(\iint \mathbf{Adup}\right)_{\mathbf{ni}} + \left(\iint \mathbf{Adup}\right)_{\mathbf{tuo}} \tag{15.5}$$

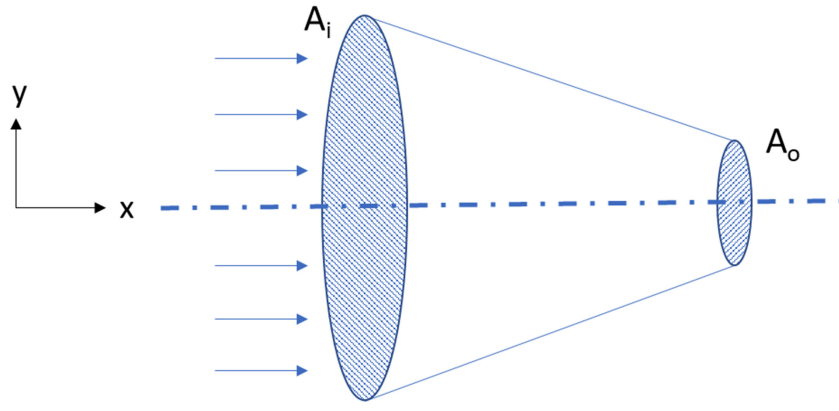

Figure 15.1. Schematic for variable area channel.

For steady state flow, the mass flow rate at inlet and outlet are equal. The average velocity, $\bar{u}$ is an equivalent uniform velocity that could give the same volumetric flow rate as that induced by variable velocity.

$$\bar{\mathbf{u}} = \frac{\iint \mathbf{A}\mathbf{d}\mathbf{u}}{\mathbf{A}} \tag{15.6}$$

Thus, equation (15.5) can be written in terms of average velocity as:

$$\boldsymbol{\rho}_{\mathbf{i}} \bar{\boldsymbol{u}}_{\mathbf{i}} \mathbf{A}_{\mathbf{i}} = \boldsymbol{\rho}_{\mathbf{o}} \bar{\boldsymbol{u}}_{\mathbf{o}} \mathbf{A}_{\mathbf{o}} \tag{15.7}$$

Equation (15.7) represents the continuity equation in algebraic form that is used to relate the average velocity within variable areas of channel.

The Reynolds transport theorem can be used to get a force balance equation. The momentum conservation equation or Navier–Stokes equation can be written by considering '*N*' as the momentum of fluid 'mV'. Thus, on the left-hand side of equation (15.1), the rate of change of momentum of the system gives force acting on the fluid, F_{sys}. This force on the system can be body force or surface force. Thus, using RTT from equation (15.1), we get:

$$\frac{\partial}{\partial t} \iiint \boldsymbol{\rho} \vec{\boldsymbol{V}} \boldsymbol{d} \forall + \iint (\boldsymbol{\rho} \boldsymbol{V}) \vec{\boldsymbol{V}} \cdot \boldsymbol{dA} = \mathbf{F}_{\mathbf{sys}} \tag{15.8}$$

Applying the Gauss divergence theorem and considering the arbitrary choice of elementary volume, the momentum equation for the *i*th direction can be written as:

$$\frac{\partial}{\partial \mathbf{t}} (\boldsymbol{\rho} \mathbf{u}_{\mathbf{i}}) + \nabla \cdot (\boldsymbol{\rho} \mathbf{u}_{\mathbf{i}} \vec{\boldsymbol{V}}) = \nabla \cdot \vec{\boldsymbol{\tau}}_{\mathbf{I}} + \mathbf{b}_{\mathbf{i}} \tag{15.9}$$

Equation (15.5) is referred to as the Navier equilibrium equation that explains the relationship between the rate of momentum change in control volume and forces acting on it. Here, $\boldsymbol{i}$ is the stress tensor in the *i*th direction. For Newtonian and isotropic fluid, the constitutive relation between stress and strain rate is given in terms of fluid parameters that can be measured such as velocity and pressure. Substituting that in equation (15.5), in vector form for incompressible flow, we get:

$$\boldsymbol{\rho} \frac{\boldsymbol{dV}}{\boldsymbol{dt}} = -\nabla \boldsymbol{P} + \boldsymbol{\eta} \nabla^{\mathbf{2}} \mathbf{V} + \boldsymbol{\rho} \mathbf{b} \tag{15.10}$$

This represents the Navier–Stokes equation for incompressible flow. It is important to note that the left-hand side of equation (15.6) is negligible in microfluidic applications. Thus, it is boon for us that the non-linear derivative part itself tends to zero, and thus it becomes easy to get analytical solutions for several microfluidic cases such as flow-through circular microchannel. To illustrate the application of the Navier–Stokes equation in microfluidic analysis, we consider a simple example of fluid flowing through a circular duct. Neglecting body forces, we get balance of pressure force and viscous force. Solving this momentum equation, we get the axial velocity profile for a fully developed laminar flow

$$u = -\frac{\mathbf{R2}}{\mathbf{4\mu}}\frac{\mathbf{dp}}{\mathbf{dz}}\left(1-\frac{\mathbf{r2}}{\mathbf{R2}}\right) \tag{15.11}$$

This represents the parabolic velocity profile and its variation with the radius of the duct. This expression can be used to relate pressure drop in the duct and flow rate which is given by:

$$\mathbf{\Delta P} = \frac{\mathbf{128\mu QL}}{\mathbf{\pi D4}} \tag{15.12}$$

where μ is the viscosity of fluid, Q is the volume flow rate, L is the length of the duct, D represents the hydraulic diameter. Thus, being able to get such simple expressions is helpful for first-hand calculations to design the channel dimensions for applications.

15.2.2 Surface tension and wettability phenomenon

Another perspective in the microfluidic study is to investigate the wettability of a surface. It is vital from the development of several applications as well as surface chemistry involving de-wetting and de-icing surface, droplet dynamics, inkjet printing, digital microfluidics, etc. Surface tension or surface energy is defined as the amount of work done to increase one unit's surface area. The SI unit of surface tension is *N/m*. Wetting and de-wetting of the surface depend on this crucial physical property.

Let us consider a sessile drop of liquid on a flat surface, as shown in figure 15.2. The different interfacial tensions are shown at the droplet triple contact line as γ_{lv} (liquid–vapor), γ_{sl} (solid–liquid), and γ_{sv} (solid–vapor). Applying force balance at the contact line, we get:

$$\cos\theta = \frac{\gamma_{sv} - \gamma_{sl}}{\gamma_{lv}} \tag{15.13}$$

This equation is referred to as Young's law where θ represents the contact angle. If the contact angle is less than 90°, the surface is said to be hydrophilic, and if it is greater than 90° surface is hydrophobic in nature.

Now, consider a flat surface. What will happen when you pour a few micro-liters of liquid on it? Does it form a film, or is it stable in the form of a droplet? As we know, if we have a drop in the air (with negligible gravity), it attains a spherical shape at minimum energy configuration. But here we have a solid–liquid interaction

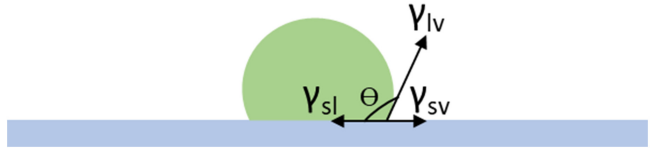

Figure 15.2. Schematic of a sessile drop on a planar substrate.

as well. Figure 15.2 shows that all the three interfacial tensions are essential to define the wetting condition based on its contact angle. Thus, the spreading parameter, S, is defined as the difference of the dry energy state and wet energy state.

$$S = \gamma_{sv} - (\gamma_{sl} - \gamma_{lv}) \tag{15.14}$$

If $S > 0$, we get total wetting, and when $S < 0$, we get partial wetting of the surface in the form of droplets. The low surface energy substrates are hydrophobic in nature and vice versa.

In microfluidics applications, we often require performing surface treatments to convert the hydrophobic surface into hydrophilic and vice versa. Generally, hydrogenated and fluorinated surfaces are used as hydrophobic coatings such as Teflon and PDMS. While in situations like PDMS microchannel, when we need to flow liquid, we plasma treat to hydrophilize the layer.

15.2.3 Non-dimensional numbers and their relevance in microfluidics

To understand the phenomenon occurring in microfluidics scale, it is important to appreciate its associated effects. Usually, in any phenomenon, two or more competing forces play a role and thus, it would better to group them as a non-dimensional form to study its effect.

1. Reynolds number (Re): refers to the ratio of inertial to viscous force. In microfluidics, Re is generally less than unity, thus the viscous force dominates over inertia. Re numbers are used to differentiate between turbulent and laminar flow and help predict different fluid flow patterns. Usually, when the Re number is less than 2000, we assume fluid flow is laminar. However, Re values greater than 2000 are taken as turbulent. In this way, the Re number is useful to control fluid pattern.

$$\mathbf{Re} = \boldsymbol{\rho} \mathbf{V} \mathbf{L} / \boldsymbol{\eta}$$

   where ρ is the liquid's density, V is the velocity, L represents the characteristic dimension, and η is the dynamic viscosity.
2. Capillary number: is defined as the ratio of surface tension to viscous force. It is relevant in the case of immiscible liquids such as droplet formations in the continuous immiscible medium. The surface tension affects the free surface dynamics.

$$\mathbf{Ca} = \boldsymbol{\eta} \mathbf{V} / \boldsymbol{\gamma}$$

3. Peclet number: defines the relative importance of convention to diffusion. This is highly important in mixing applications in microfluidics.

$$\mathbf{Pe} = \mathbf{L} \mathbf{V} / \mathbf{D}$$

   where D is diffusivity.

15.3 Device fabrication

In the previous section, we discussed micro-scale fluid phenomena and the related physics. Going forward, to perform a real experiment, we need a microfluidic device. The microfluidic device was created when progress was made in microelectronics and the MEMS industry combined with biochemical applications. The fabrication of the microfluidic device plays a vital role in its success. The design depends on the application in which it is to be implemented. There are several methods for fabricating microfluidic chips, but most common are soft lithography, micro-machining, and 3D printing. We will discuss each of these to give a complete picture. Depending on the requirements, the user can opt for specific methods.

15.3.1 Soft lithography

This is an important technique for fabricating microchannels and creating micro/nanostructures onto a surface or inside a microchannel. This technique was developed by Whitesides group that involves a soft polymeric mold such as a PDMS replica from a hard master [6]. The master mold is prepared using photolithography on silicon generally. Several polymers are being used to fabricate microfluidic channels such as PDMS (most popular), photocurable perfluoropolyether, photosensitive polymers, and polymerized hydrogels.

An integrated microfluidic device contains a channel layer bonded to either a micro/nanostructured layer or plane surface like glass. To fabricate a channel (figure 15.3), prepolymer PDMS (10:1 silicone elastomer and curing agent, the ratio depends on the stiffness of channel required) is cured on the master mold (generally made of SU8 or Si using photolithography) by keeping it at 70 °C–80 °C for 1 h approximately. After the polymer is fully cured, it is removed from the master mold and bonded with a cleaned glass substrate using plasma treatment. This simple bonding without high temperature or pressure makes multiple layer stacking easier

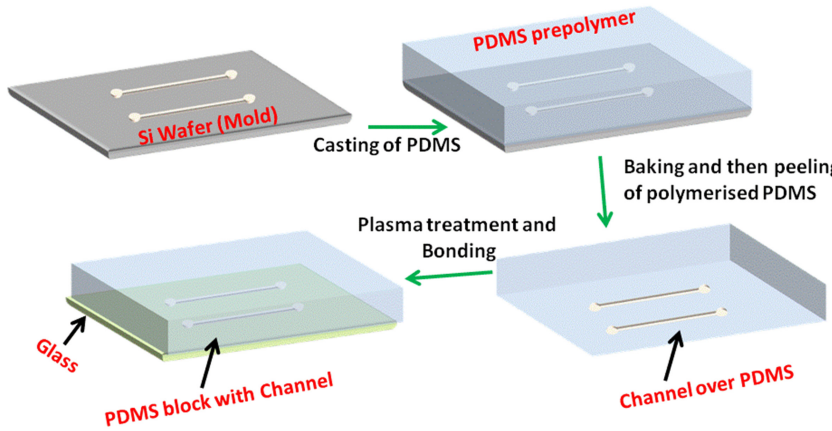

Figure 15.3. Schematic representation of microchannel fabrication with PDMS using soft lithography.

(as in multilayer soft lithography used to create PDMS valves). The important thing to note is that the silicone elastomer ratio to curing agent varies with applications such as multilayer stacking, valves, or pumps. It is also important to note that with multiple uses, device performance reduces due to surface adsorption by some biomolecules from sample or impurities present. To solve this issue, the substrate (the surface to which channel is bonded) is modified using PEG (polyethylene glycol) to prevent biofouling.

There are two soft lithographic methods to create micro/nanostructures on a surface or inside microchannels—contact printing and capillary molding [7]. Contact printing is generally used to generate a chemically modified surface, while capillary molding is used to create topographical-modified physical micro/nanostructures. In contact printing, direct printing is done using an elastomeric stamp, as shown in figure 15.4(a). Once the stamp is cured, it is soaked in the 'ink' to be printed and brought into conformal contact with the substrate where it is to be printed. It is beneficial for low-cost batch production but generally used for 1D patterns. The resolution of such techniques is 500 nm and can go as high as 50 nm with hard PDMS mold. The capillary molding method generates 2D structures on the surface. In this technique, an elastomeric mold (PDMS or PUA) is placed on the polymer surface (figure 15.4(b)). It is then heated above its glass transition temperature due to which capillary force makes polymer flows in the void created between mold and polymer layer. It is also possible with UV curable resin followed by solvent evaporation. The resolution of such a technique is up to 50 nm in PUA mold.

This polymer-based soft lithography process has largely revolutionized microfluidic device fabrication as it enables fast, inexpensive manufacturing with a broad range of polymer materials.

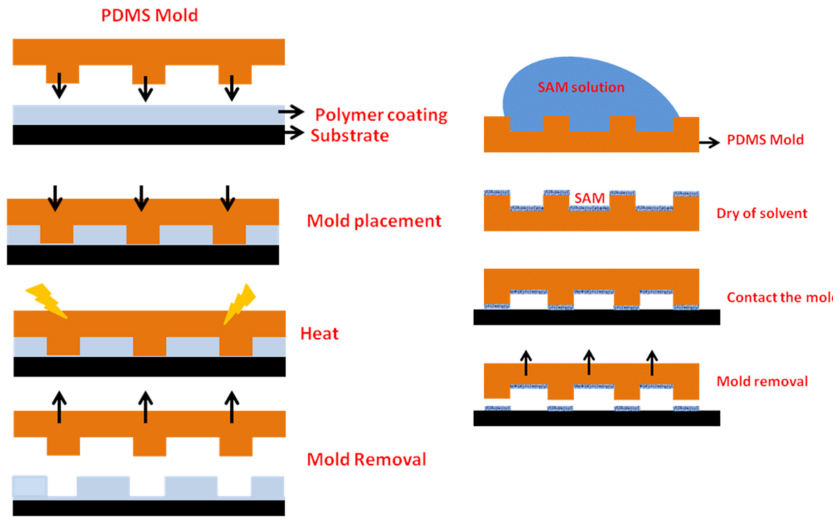

Figure 15.4. (a) Capillary molding and (b) contact printing.

15.3.2 Micromachining

Another approach to fabricate microfluidic devices is the micromachining of glass/Si substrate. There are several advantages of glass and silicon substrates such as thermal stability and solvent resistance, making it an appropriate choice for microfluidic chip fabrication. Typically, micromachining constitutes three steps—photolithography, etching, and bonding.

In the photolithography step, the substrate is cleaned and spin-coated with photoresist (PR). There are two types of PR being used, namely positive and negative. The positive PR is one in which the portion exposed to light becomes soluble to the developer, and in negative PR, the light-exposed part becomes insoluble. The soft bake temperature and duration after the PR coating depends on the type of PR used. After exposure through a photomask (containing microchannel design) in the lithography tool, the pattern is transferred to the PR layer. It is then developed in a photoresist developer to wash away the rest of the PR region. Depending on PR, it is followed by a hard bake. The desired microchannel design is now on the PR coated substrate. This PR layer helps in selective etching the substrate using etchants. Next, PR is inert to the etchant, thus creating microchannels on the substrate. The PR layer is later removed from the substrate. After the etching step, we get an open microchannel on the substrate needed to be bonded to another substrate to close it using thermal or adhesive bonding.

However, the rigidity of substrate, gas impermeability, high cost, and need for cleanroom facilities restrict this method's use for large-scale production.

15.3.3 3D printing

This is a relatively new technique being used. As the structure complexity increases, time and cost of fabrication also go up. It also hinders the automated system for fabrication. Thus, generating 3D structures in a single step is beneficial for rapid and high-throughput manufacturing. In this approach, 3D geometrical information is stored in a computer as a CAD file that runs the attached printer.

Stereolithography (SL) is one of the most popular types of 3D printing used to fabricate microfluidic channels. It polymerizes the photocurable resin layer by layer through laser irradiation. The laser beam is focussed and scanned over the liquid resin's surface for the liquid–solid transformation of the layer, thus creating the structure. The fresh resin is then spread over it, and again light-induced solidification occurs, creating complete 3D structures. There are other 3D printing methods like multi-jet modeling use inkjet printers to create 3D structures and fused deposition modeling in which layers of thermoplastic polymer are deposited using a heated extrude nozzle.

This technique enables fabricating accurate design in one step with acceptable resolution and offers less time and labor cost. Unlike soft lithography and micromachining, 3D printing is an additive manufacturing method that interfaces with an industry grade user interface and embedded control system for large-scale production.

15.4 Biomedical applications of microfluidics

Unil now, we have discussed microfluidics physics and device fabrication methods. One more critical aspect that one should know while developing a microfluidic platform for biomedical applications is the flow control system. Once we fabricate a microchannel say by soft lithography and bond it with the glass substrate, we need to know about flow actuation mechanisms and interfacing with external pumps via tubes.

Flow is generally manipulated using a syringe pump that controls the flow rate. It is a favorable way to actuate liquid as flow rate can be altered directly by changing the stepper motor's speed. It is important to note that it takes a little time for the flow to stabilize when you change the flow rate due to fluctuations in flow rate supplied and pressure [8]. Since the PDMS microchannels are flexible they offer compliance. Researchers have used a flow reduction mechanism to benefit from this case and tried to control the liquid interface movement with high resolution by using feedback control to the input signal. There is another aspect of using elastomeric valves [9] in the microfluidic channel to control the flow rate. Researchers have developed a multilayer soft lithography method to fabricate PDMS check valves where the pneumatics is used to actuate the valves depending on dimensions.

So far, we have chronologically discussed the area of microfluidics explaining its physics and device fabrication methods. However, several specifics need to be discussed as per the applications they are suited to. We will briefly cover such aspects and discuss the role of microfluidics in their respective applications. The design of microfluidic channels depends on the application. This section will discuss some of the major biomedical research areas where microfluidics offers significant experimental advantages over conventional methods to biologists. From fundamental research to the development of a portable diagnostics kit, there is a range of examples from current research to give readers a broad perspective and help them understand the real benefits of microfluidic devices in biomedical applications.

15.4.1 Microfluidics for single-cell analysis

Cells are the basic unit of living organisms. The bulk cell assays provide information, but the average data obtained neglects the differences in intracellular molecular expressions from individual cells due to cell heterogeneity. This leads to the loss of vital data during averaging. The single-cell assays reveal heterogeneities in cell morphology, functions, composition, and genetic performance. However, there are certain challenges in single-cell analysis—owing to the small size of most cells, manipulation is difficult in conventional bulk sample preparation strategies; small concentration of sample demands more sensitive detection methods. With the advances in microfluidics technology, it provides a solution to the above challenges. The micrometer-size channels and physical structures comparable to cells make single-cell manipulation efficient. The microfluidic chips can integrate multiple functionalities such as cell isolation, cell lysis, and cell analysis with detection methods available on-chip.

This section will discuss single-cell manipulation methods on microfluidic chips and applications like characterizing the mechanical and electrical properties of cells.

15.4.1.1 Single-cell isolation

The first step in single-cell analysis is cell isolation. Individuals cells are isolated in an enclosed chamber to separate them. The cell sorting technique should detect cell-type-specific markers, sort cells at single-cell resolution, and maintain cell viability. There are different techniques available such as mechanical traps, droplet traps, and active forces like hydrodynamics trap, DEP trap, magnetic trap and acoustic trap. Figure 15.5 shows trapping of micro/nano scale particle by hydrodynamic forces.

15.4.1.2 Single-cell lysis

Cell lysis occurs when the cell membrane (and/or cell wall) is disrupted, allowing cytoplasm content to be released. There are four methods that are being used for cell lysis—mechanical, chemical, electrical, and thermal. The use of mechanical force is one of the most common ways to puncture the membrane. In microfluidic devices, cells are forced to pass through a filter with an opening too small to pass the whole cell, thus shearing the cell membrane. Another method utilizes a PDMS membrane in a microfluidic channel to crush the cell membrane.

In the thermal cell lysis method, cell samples are heated at high temperatures. This method is generally used in PCR-based assays. In chemical lysis, buffers, or other lytic reagents (surfactants) are used to break the cell membrane. The cell sample flowing in a channel is mixed with cell lysis agents, then made to flow through a sufficient long channel giving it sufficient diffusion time. The mixture is then separated at T-junction, where lysed cells and lytic agents are separated. Exposure of cells to a high electric field is sufficient to cause cell lysis. As the pulse

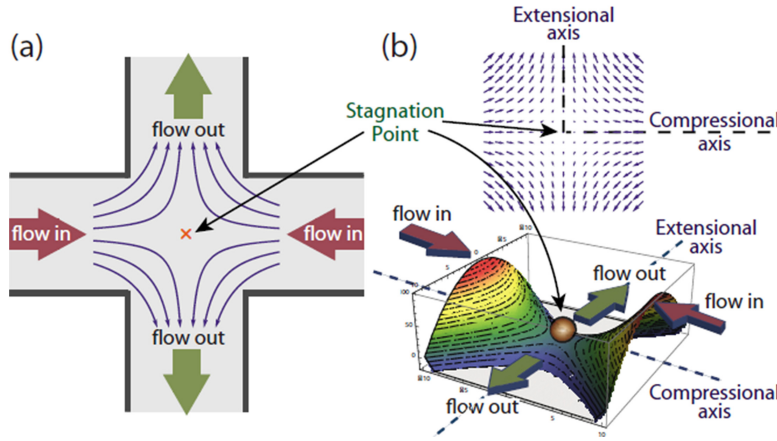

Figure 15.5. Hydrodynamic trap created by two laminar inlet streams which converge at a channel junction and two divergent outlet streams in the opposite direction perpendicular to the inlet. This geometry creates a planar extensional flow which contains a stagnation point or point where velocity is zero (at the center of the channel junction). Reprinted from [10], with the permission of AIP Publishing.

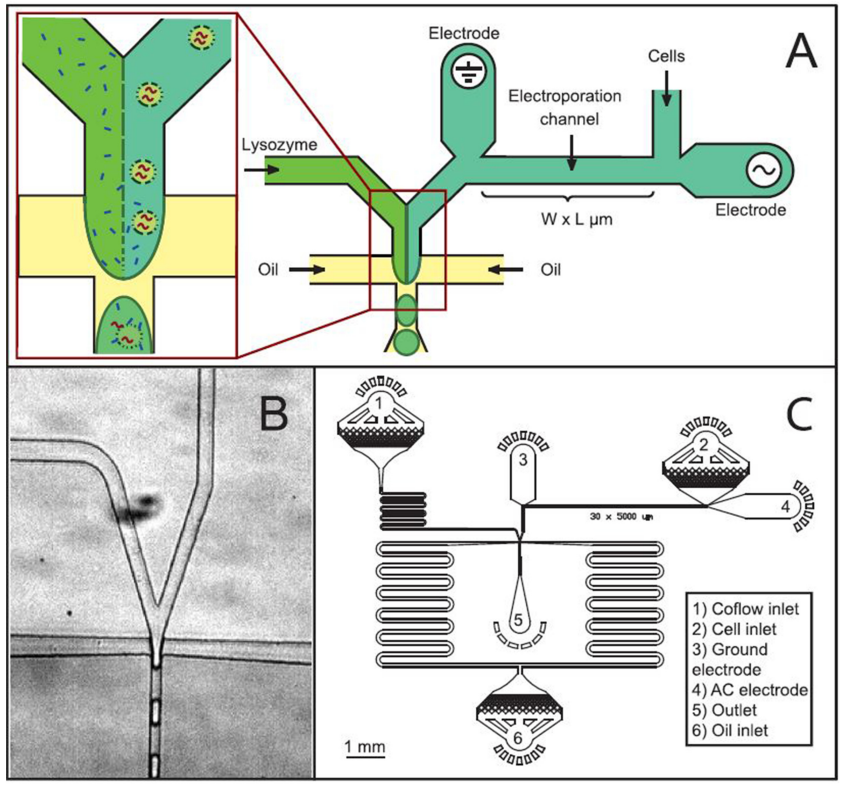

Figure 15.6. The schematic diagram of electrical lysis for droplet screening. (a) Representation of electrical lysis and droplet generation part. (b) Image of the droplet generation. (c) Design of the complete lysis device with electroporation channel having dimensions of 30 μm × 5000 μm. Reprinted from [11], with the permission of AIP Publishing.

length and electric field strength reach a critical value, cells are lysed by dielectric breakdown of the cell membrane (figure 15.6). In microfluidic devices with integrated electrodes, cell lysis can occur at low voltage due to the smaller distance between electrodes and high field strength than a conventional setup requiring 500 V.

15.4.1.3 Mechanical and electrical property of cells

The electrical properties of the cell membrane and cytoplasm and the cytoskeleton's mechanical properties determine the overall biophysical properties of cells [12]. There are different microfluidic devices based on patch-clamp, electro-rotation, and micro-electrical impedance spectroscopy (μ-EIS). The patch-clamp devices characterize cellular ion channel activities by sucking a cell membrane into a micro-pipette to form a high electrical resistance seal. This technique disrupts the cell membrane and hence cannot be used for long-term study. The rotating electric field exerts a force on a suspended cell to rotate due to Maxwell–Wagner polarization

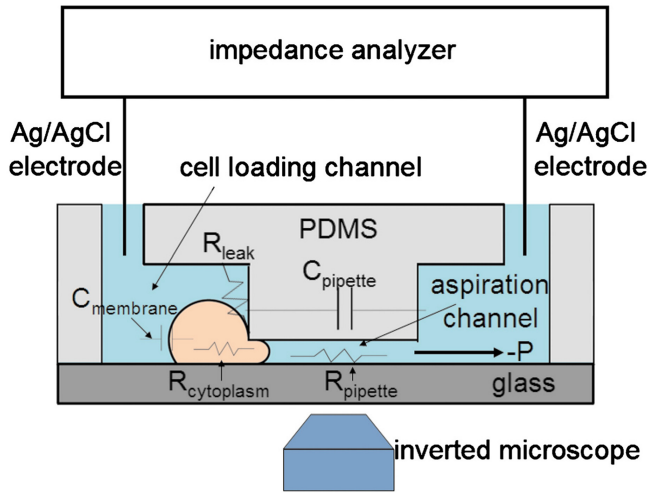

Figure 15.7. Electrical and mechanical characterization of a single cell that is trapped by applying negative pressure. Impedance measurement is conducted by two Ag/AgCl electrodes. Reprinted from [12], with the permission of AIP Publishing.

in electro-rotation devices. In the μ-EIS device, a frequency-dependent signal is applied across a single cell to measure the corresponding current. The microfluidic device with constriction is used to measure the deformability and Young's modulus of cells. Figure 15.7 shows impedance measurement during single-cell entrapment in a constricted micro-channel. Other methods incorporate electro deformation, micro-pipette aspiration, and optical stretcher to measure the mechanical properties of cells.

Apart from mechanical and electrical properties, with the development in microfluidic technology, it is used for studying cell–cell interaction, cell genetic and protein analysis, and diagnosis.

15.4.2 Microfluidics-based PCR devices

Among the microfluidics, the miniaturized PCR instrument (or PCR microfluidics) has become a valuable tool for molecular biology since it can potentially help deoxyribonucleic acid (DNA) amplification. In general, the PCR cycle involves three distinct steps: denaturation, annealing, and extension. In the denaturation step, the temperature rises to ~95 °C; thus, two single strands are denatured from a double-stranded DNA. Next is an annealing step where the primer binds with the target DNA sequence, and the temperature decreases to ~56 °C. Further, in extension steps, DNA polymerase attaches free DNA nucleotides available in solution to template DNA at 72 °C. This activity synthesizes second complementary DNA from free nucleotides in solution. Therefore, the three repetitive steps are necessary to efficiently increase double-stranded DNA concentration. In this context, microfluidics is revolutionizing the way lab-testing procedures are conducted especially for applications accounting in PCR devices. PCR microfluidics of

varying design have been developed for effective and fast DNA amplification and are broadly classified as chamber stationary PCR, flow-through PCR, and thermal convection-driven PCR [13]. The chamber stationary PCR works in a conventional manner, that of a normal PCR device, where the solution is kept stationary and the temperature of PCR reaction chamber is cycled between the above mentioned three temperatures. The amplification products upon completion are recovered for either off-line detection or are detected online. Unlike chamber stationary PCR, flow through PCR configures its microfluidics devices with a 'time-conversion concept' wherein the PCR solution is continuously flowing through three different temperature zones necessary for amplification instead of making it stationary. This approach however, is more flexible to change the reaction rate resulting in reduced cycling and heating time. Next, convectively driven PCR microfluidics in its rudimental stages is capable of rapid DNA amplification. The designs for convection-driven PCR devices employs only two temperature zones which facilitates sample flow, resembles flow-through microfluidics to a certain extent. By employing Rayleigh–Benard convection to perform PCR amplification inside a cylindrical cavity measuring 35 μl and continuously shuttling fluid vertically between two temperature zones such that, annealing/extension was above 61 °C and denaturation was below 97 °C. Subsequently, laminar convection comprises a layered PCR which facilitates a cheap reaction chamber with a high reaction speed using a non-contact heating method. PCR microfluidics consists of a chamber with a diameter of 5 mm and thickness of 1 mm heated in the center of the chamber by an infrared source. This design of PCR cycles a volume of 20 μl and achieve a 1 000 000-fold DNA amplification. Convectively driven PCR microfluidics are very simple in their design, have the advantages of cheap fabrication and much faster temperature transition speed.

Further, a polyimide microfluidic device was designed for 30 cycles of PCR with a time ratio of 1:1:2 for denaturation, annealing, and extension step as presented in figure 15.8. Similarly, a design featured 30 cycles of PCR in a polycarbonate substrate using a computer numerical controlled (CNC) vertical milling machine. In this study, however, temperatures were created using two copper heating blocks for denaturation and a combined annealing/extension step. Additionally, to reduce flow resist of these devices, Wu *et al* coated a 0.5 mm inner diameter steel capillary with Norland Optical Adhesive 61 (NOA61) [14]. The above examples implement different materials to simplify the design of these devices and discuss flow resistance optimization. Due to the low cost of plastic devices, they can be disposed of almost immediately in order to avoid cross contamination arising through absorption of DNA onto the channel walls. It is the miniaturization of PCR devices that can offer an opportunity to improve them further in terms of shorter amplification times, higher sample throughput, and by extension result in minimum human/world-to-PCR intervention and contamination. In other words, some advances may contribute to making the operations of these devices simpler and more robust, while others may significantly compromise the purpose of this equipment.

Through a wide array of techniques, microfluidics offers several options for performing digital PCR either by creating droplets or microwells. In comparison, a

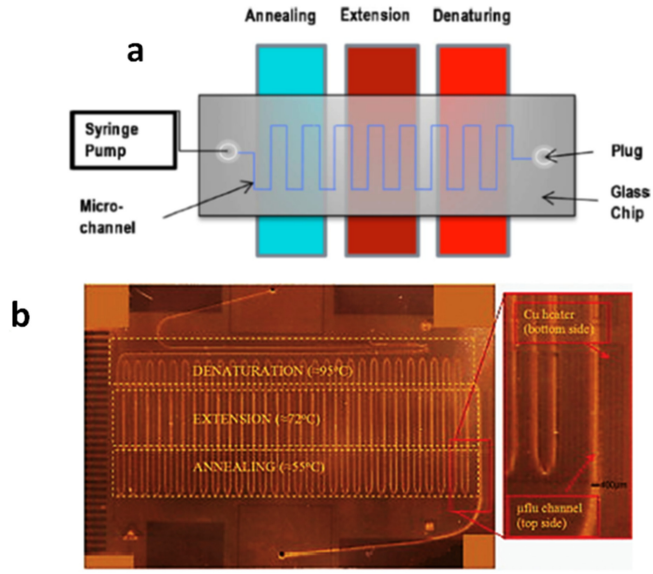

Figure 15.8. (a) Schematic representation of PCR-based microfludics device integrated with heater for denaturation, extension and annealing steps. Reprinted from [15], with the permission of AIP Publishing. (b) A serpentine based microfluidics device using three copper heaters. Reprinted from [16], Copyright (2014), with permission from Elsevier.

droplet of PCR showed a high sensitivity consistent with the standard methods [17]. Additionally, digital PCR spotted minute differences which even the qt-PCR (quantitative PCR) could not detect. For instance, Floren *et al* used digital PCR to identify several different species and were able to correlate tissue samples and the amount of mitochondrial DNA [18]. In another study by Hoshiona *et al* in his quantification of DNA from soil samples, qrt-PCR (quantitative reverse transcription-PCR) underestimated the DNA content due to inhibition, however, digital PCR showed more resilience [19]. Furthermore, isothermal nucleic acid amplification methods show a higher robustness against temperature variations and inhibition compared to conventional PCR. Microfluidics PCR systems for sample preparation and detection avail compartmentalization of DNA molecules into individual volumes from bulk solution. Due to its precise fluid control nature and reduced fabrication costs combination, it can be therefore inferred that isothermal nucleic acid amplifications using PCR microfluidics are providing a pathway for point-of-care applications.

15.4.3 Biosensor integration in microfluidic systems

According to IUPAC, a biosensor is defined as an independent integrated receptor transducer device, which can provide selective quantitative or semi-quantitative analytical information using a biological recognition element. On the other hand, the microfluidic system offers precise control over fluid flow in microscale volume.

Thus, it is another on-going research area to integrate biosensors on the microfluidic chip to achieve reduced sample consumption, portability, multiplexed detection, and low-cost point-of-care devices.

The biosensor has mainly two-components, the biological and physical. The biological components are basically enzymes, nucleic acids, antibodies, etc, that are collectively called bioreceptors and are known for their specific binding capability with analytes/markers. This bioreceptor is immobilized over the transducer surface (physical component), which produces physical and chemical changes after interaction between the bioreceptor and analyte. These signal changes are further amplified, processed, and interpreted also for display in suitable units. As we discuss there are different biological recognition sensing elements such as enzymes, aptamers, and antibodies employed to define selectivity and specificity and decrease the possibility of interference with undesirable substances. Enzymes are proteins that catalyze chemical reactions, typically redox reactions when used as biosensors. Antibody-based biosensors have also become popular after monoclonal antibody technology developed by Kohler and Milstein. Aptamers are amino acid polymers or a single-stranded nucleic acid that can bind to their specific ligands with a dissociation constant in the micromolar to picomolar range. Biosensors can also be classified based on their transduction mechanisms—electrochemical, optical, and mechanical.

15.4.3.1 Enzyme-based biosensor on a microfluidic platform

There have been several efforts to integrate biosensors with microfluidic chips. Glucose and urea levels in the blood have been measured using integrated chips. One such work is in the droplet microfluidics-based electrochemical sensor [20] to sense glucose level in human blood serum.

A platinum-black microelectrode (working electrode) was used for glucose sensors in flowing droplets. As shown in figure 15.9, the tapered capillary tip containing buffer and sample is connected to the PDMS chip. The sample stream is combined with GOx (glucose oxidase) enzyme and substrate glucose.

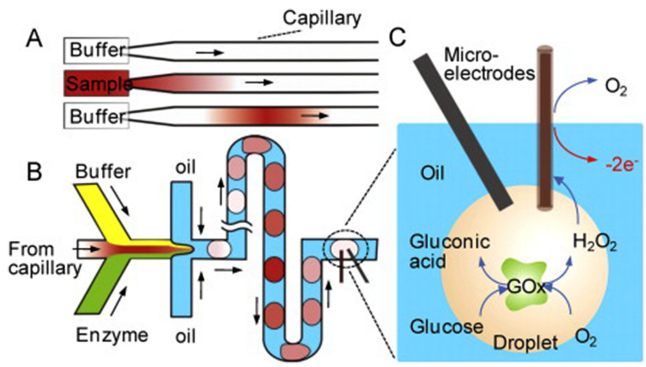

Figure 15.9. Schematic diagram representing the electrochemical sensing of glucose in droplets. Reprinted from [20], Copyright (2014), with permission from Elsevier.

By maintaining a suitable flow rate of mineral oil, the droplet is formed inside the microfluidic channel. The activity of GOx is estimated by measuring H_2O_2 concentration on the Pt-black electrode at the end of the microchannel.

15.4.3.2 Antibody-based biosensor on a microfluidic platform

The integration of a continuous microfluidic device and biosensor using antibodies as the biological recognition element is demonstrated to detect breast cancer using the surface plasmon resonance (SPR) phase imaging method [21]. An automated lab-on-a-chip microfluidic biosensor with multiple channels for the detection of microarray samples is developed (figure 15.10). Since SPR is a temperature-dependent technique, a temperature control unit consisting of micro heaters and temperature sensors to avoid temperature change and variation in the sensing area is used. A regular self-assembled monolayer (SAM) was used to immobilize the anti-rabbit IgG on the modified gold surface. The results showed that the fabricated microfluidic platform, which used SPR phase imaging successfully detected the presence of only IgG in the samples. Similarly, many other applications are reported in the literature on antibody-based biosensor in microfluidics platforms.

15.4.3.3 Aptamer-based biosensor on a microfluidic platform

An on-chip aptamer-based sensor was developed for the continuous detection of transforming growth factor (TGF-β1). The microdevice was fabricated on a glass substrate with gold electrodes and two PDMS layers (figure 15.11). The two PDMS

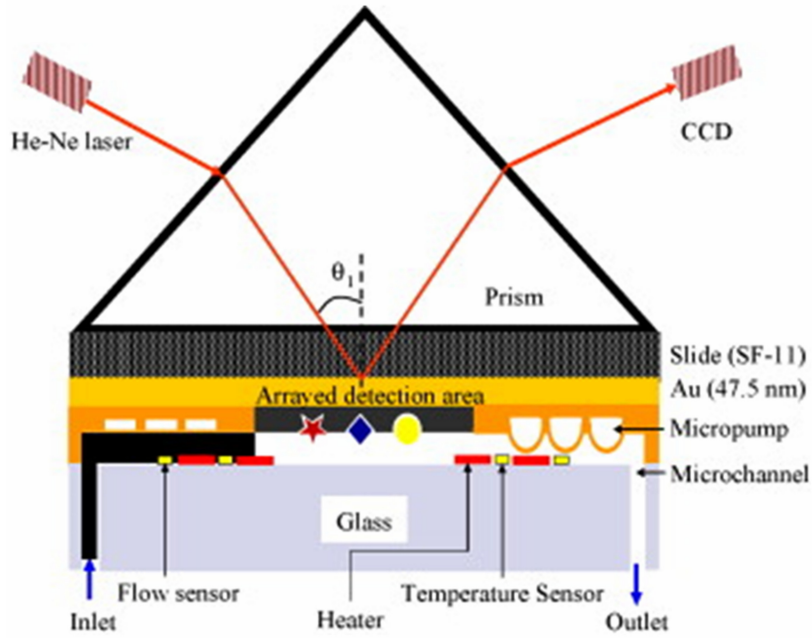

Figure 15.10. Microfluidics integrated SPR imaging system for detection of a microarray immunoassay. Reprinted from [21], Copyright ((2007) with permission from Elsevier.

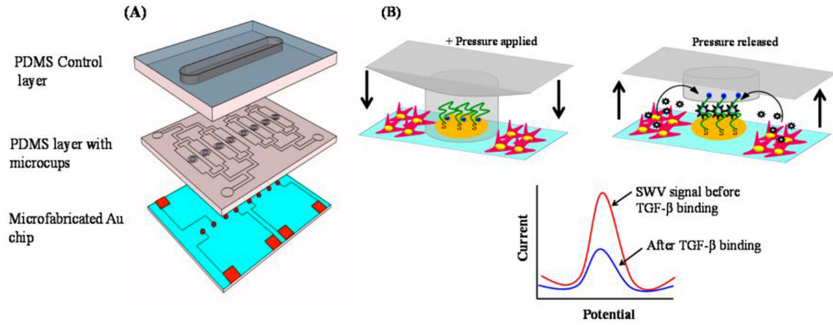

Figure 15.11. Aptasensor integrated microfluidic device for transforming growth factor from liver cells. (a) Schematic of a three layer microfluidic device. (b) Actuation of microcups to protect electrodes during collagen coating. Reprinted with permission from [22]. Copyright (2014) American Chemical Society.

layers were designed so that the first layer contains microchannels and semi-circular microcups, and the second layer was mainly used for pneumatic control. The microcups were raised during the protein secretion by cells which increased protein diffusion toward the sensing area. The microcups were then lowered during the physical separation of cells from the sensing electrode area. Square wave voltammetry (SWV) measurements were used to confirm the interaction between the cell-secreted protein (TGF-β1) and the specific aptamer. The results showed a decrease in the redox signal, which is proportional to the sample's analyte concentration.

15.4.4 Microfluidics for organ-on-chip technology

Conventionally 2D cell culture is being used to study cell microenvironment and chemicals' effects on cellular response. But it is not very reliable as it does not support tissue-specific functions of cell types and does not mimic *in vivo* conditions. This has led researchers to 3D spheroid-based studies that usually rely on hydrogels, comprised of natural or synthetic polymer extracellular matrix (ECM). It is being used to study cell–cell interactions. However, it also has limitations such as 3D spheroids being variable in size and shape; thus, it is difficult to maintain consistent cell positions for analysis. It also lacks multiscale arrangements of the tissue–tissue interface, such as between vascular endothelium and connective tissues. Fluid flow condition is absent as it is *in vivo* due to circulating blood and the effect of shear stress and interaction with immune cells necessary for healthy body organs. Thus, microfluidic chip-based technique (organ-on-chip) [23] to mimic body physiology offers the possibility to overcome these limitations. It can be referred to as living cells culturing device in continuously perfused chambers to mimic functional level similarities at the tissue and organ level. Researchers have been working in this area with several perspectives like the simulation of cancer model on-chip to study its complex mechanisms for metastasis; vascular-on-chip is another hot area to mimic blood capillaries on a microfluidic chip; development of body-on-chip to recapitulate parts like lungs [24], brain [25], gut, kidney [26], heart [27] on a single platform with a vision for fundamental research and originating the concept of

personalized medicine. This section will first discuss the organ-on-chip concept and how it is being used to study organ-level functionalities and physiology, followed by a brief discussion on biocompatible materials as an alternative to PDMS for cell culture. In the later part, we will highlight vasculature-on-chip and cancer-on-chip technologies and their current research status.

With the advent of soft lithography fabrication, microfluidic chips have been seen as a better alternative for cell culture. It provides control over several system parameters that are important in cell culture-based study. It consists of creating a miniaturized perfused channel in which ECM molecules are coated on the surface, followed by the flowing of the cell medium so that cells adhere to ECM coated substrate. Continuous perfusion is being done with the culture medium. The PDMS-based cell culture system being optically transparent, allows real-time optical imaging of cell response to environmental cues. Microsensors can be integrated into the microfluidic chip to analyze cell migrations, tissue barrier integrity, and fluid pressure. Microfluidic devices being a laminar regime flow helps in creating physical and chemical gradients that have assisted researchers in studying directional cell migration, cardiac tissue formation, nerve axon outgrowth, and cell–cell junctional integrity. These devices also offer controlled cell patterning with different types of cells. The ability to integrate a porous substrate between two microchannels (having different cells) has enabled the study of tissue interfaces that mimic vascular endothelium and parenchymal tissues. These microfluidic chips are also useful in creating a complex mechanical microenvironment that can simulate cyclic strain and fluid stresses that are somewhat like what cells experience in breathing and cardiovascular cycling.

Although most organ-on-chip studies are related to established cell lines, it can be used for plant cells or even stem cells study. Researchers have also investigated induced pluripotent stem cells because of the potential to model diseased organs with patient-specific cells. These lines of research are directed towards personalized human-on-chip. Researchers have fabricated chips to study liver, kidney, intestine, heart, lung, skin, blood vessels, brain–blood barrier, bones, and several other disease models like cancer. To provide a better understanding of this research area, we will discuss microfluidic chips for mimicking blood vessels and cancer models.

15.4.4.1 Vasculature-on-chip

The vascular system is found throughout the body, in contact with different organs and tissues. The abnormal functions can lead to several acute diseases like tumor angiogenesis and blood vessels related disease. Thus, it is crucial to develop a vascular system [28] on chip to understand *in vivo* conditions. There are four main methods to fabricate blood vessel-like microchannels on a microfluidic chip.

1. Microfluidics membrane and ECM-based devices: Depending on whether the endothelial monolayer is cultured on a membrane or an ECM, researchers have fabricated two designs. In membrane-based devices, endothelial cells are cultured on a horizontal membrane, which separates two channels, while in an ECM-based device, it is cultured on extracellular matrix sidewalls.

Membrane devices are used to measure the barrier properties of endothelial monolayers. The integration of electrodes in channels assist in the measurement of transendothelial electrical resistance (TEER). The narrow-spaced PDMS pillars are used to confine ECM between two channels. Growth factors can be introduced in channel or ECM directly to create a gradient.

2. 3D template-based models: This involves casting an ECM material around a removable template. A rod is inserted in the PDMS housing, which defines the position for microvessel structures. A solution of ECM (collagen-containing cells) is introduced around the template. Once it is cross-linked, the template is removed. The cylindrical channel network thus formed can be used for perfusion after seeding endothelial cells inside. This technique generates a vessel diameter greater than 50 μm.
3. 3D bioprinting: Liquid droplets containing hydrogels, cells, ECM proteins, and other biochemical cues are dispensed using nozzles to print a vascular array. In direct printing, a solution of ECM material and a suspension of endothelial cells in a dissolvable matrix precursor are required. Gelatin containing ECs is printed as a cylinder in a collagen ECM. The device is rotated and heated at 37 °C to dissolve gelatin. Proliferation and spreading of ECs result in the vessel lumen.
4. Self-assembly: The guided capillary self-organization method is used to create a network of capillaries in a microfluidic chamber filled with ECM. In this method, a series of diamond-shaped chambers is connected to establishing chemical and pressure gradients. The design of the microfluidic device allows the pressure difference between the source and sink through ECM. Endothelial cells are mixed in fibrinogen and thrombin ECM and the pipetted into the chamber. Under constant pressure, interstitial flow is initiated and leads to the self-organization of cells in the form of capillaries in about three weeks.

The vasculature-on-chip study is important for studying endothelial dysfunction, cancer, drug screening, and organ regeneration. Endothelial dysfunction causes thrombosis, atherosclerosis, and inflammatory diseases. Tumor angiogenesis and cancer metastasis are two important studies related to blood vessels. Reconstruction of the blood–brain barrier (it regulates the transport system between and brain and blood) and lymphatic system are another aspect of the on-chip vascular study.

15.4.4.2 Cancer-on-chip

This is another hot area of research related to organ-on-chip technology to mimic the tumor microenvironment and study cancer metastasis [29]. Controlling fluid flow, generating biochemical gradients, and incorporating mechanical cues are being done on a microfluidic platform to study different cancer progression aspects. Apart from cancer cells' genetic characteristics, its microenvironment plays an essential role in understanding this deadly disease's fundamentals. Thus, researchers have been investigating mimicking it on a microfluidic chip.

There are four important factors that are essential for developing a cancer model on-chip. They are biochemical cues, other types of cells in the tumor environment, ECM,

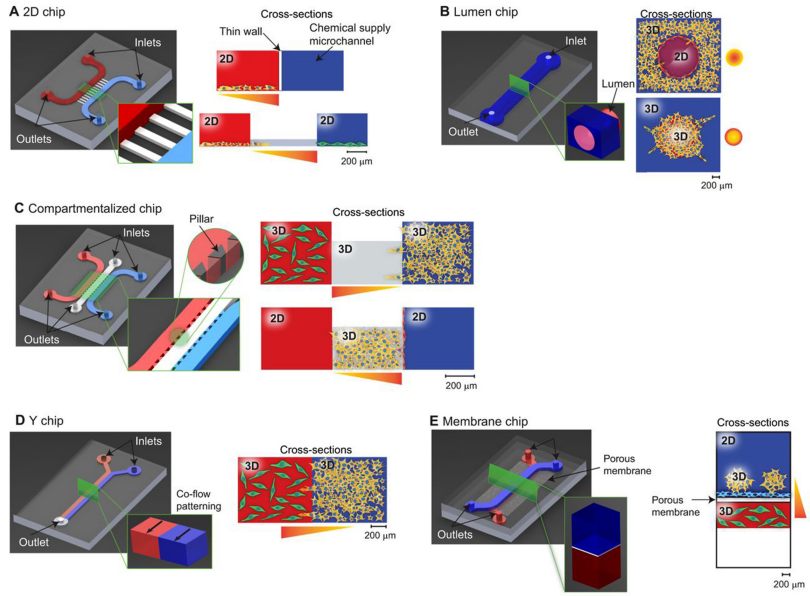

Figure 15.12. Schematic representation of different types of cancer-on-chip designs with different cell culture options [29], adapted under the terms of the CC-BY creative commons license. Copyright 2018 The Company of Biologists Ltd.

and mechanical cues. In short, we can say that these four factors comprise the tumor microenvironment. Researchers have developed different types of cancer-on-chip designs to incorporate the above four factors (figure 15.12). Generally, studies have been made concerning one factor at a time, as it is difficult to fabricate a complete microenvironment device. This is still an on-going research area. Different types of designs like 2D chips, lumen chip, compartmentalized chip, Y-chip, and membrane chip have been fabricated to study cancer-on-chip. 2D chips are single- or multi-chamber 2D culture devices with a controlled solute gradient. In this type of chip, cancer cells are typically exposed to a gradient of a solute, such as oxygen, while their viability or migration is measured. In a lumen chip, a patterned 3D matrix is used to form lumens or tumor compartments. This design is typically used to model blood vessels in tumors, or to tightly pack cancer cells in a cylindrical compartment. Compartmentalized devices use pillars to separate microchannels in which cell culturing is possible in both 2D and 3D. This type of chip is very versatile, allowing the user to pattern different matrix materials and cells in a controlled manner. The Y-chip comprised of parallel matrix compartments patterned by co-flow. This type of chip resembles the compartmentalized chip, as it enables matrix patterning, but is slightly less versatile in its patterning possibilities. In membrane chips, a co-culture device with stacked microchannels is separated by a porous membrane. One of the interesting features of these devices is that a 3D culture is created only in part of the microchannel, with the rest empty to refresh the media. This multi-layered chip type was originally developed to mimic the endo- and epithelial cell layers found in the lung.

15.5 Conclusion

Microfluidics technology has been a boon for several research areas that require fluid manipulation at a small scale. This chapter aims to provide overall knowledge and make readers acquainted with many beneficial applications of microfluidics systems. We have explained the physics of micro-scale flows and wettability effects that are important in microfluidics. We also explained fabrication methods for such microfluidic chips that are being used for several biological applications. In the last section, we have tried to highlight the use of microfluidic devices in single-cell analysis, PCR-based study, biosensor integration, and organ-on-chip technologies. In other words, a microfluidic device can be called a 'lab-on-chip' that perform whole biological assays with reduced sample consumption, enhanced sensitivity, and automation. We understand that it is not possible to discuss every aspect of such platforms in detail in a single chapter; therefore, we have cited respective papers for readers, in case they would like to investigate further in a domain. For the past two decades, microfluidics research has increased tremendously, helping biologists explore and discover a new horizon in biology. However, this technology is still to be utilized to its maximum potential. In the words of renowned physicist Richard Feynman, 'there is plenty of room at the bottom,' and this is true for microfluidic systems as well.

References

[1] Shang L, Cheng Y and Zhao Y 2017 Emerging droplet microfluidics *Chem. Rev.* **117** 7964–8040

[2] Samiei E, Tabrizian M and Hoorfar M 2016 A review of digital microfluidics as portable platforms for lab-on a-chip applications *Lab Chip.* **16** 2376–96

[3] Beyssen D, Le Brizoual L, Elmazria O and Alnot P 2006 Microfluidic device based on surface acoustic wave *Sensors Actuators* B **118** 380–5

[4] Zhang Y and Nguyen N-T 2017 Magnetic digital microfluidics—a review *Lab Chip.* **17** 994–1008

[5] Mugele F and Baret J-C 2005 Electrowetting: from basics to applications *J. Phys. Condens. Matter* **17** R705

[6] Zhao X-M, Xia Y and Whitesides G M 1997 Soft lithographic methods for nano-fabrication *J. Mater. Chem.* **7** 1069–74

[7] Kim P, Kwon K W, Park M C, Lee S H, Kim S M and Suh K Y 2008 Soft lithography for microfluidics: a review *Biochip J.* **2** 1–11

[8] Zeng W, Jacobi I, Beck D J, Li S and Stone H A 2015 Characterization of syringe-pump-driven induced pressure fluctuations in elastic microchannels *Lab Chip.* **15** 1110–5

[9] Unger M A, Chou H-P, Thorsen T, Scherer A and Quake S R 2000 Monolithic microfabricated valves and pumps by multilayer soft lithography *Science* **288** 113–6

[10] Tanyeri M, Johnson-Chavarria E M and Schroeder C M 2010 Hydrodynamic trap for single particles and cells *Appl. Phys. Lett.* **96** 224101

[11] De Lange N, Tran T M and Abate A R 2016 Electrical lysis of cells for detergent-free droplet assays *Biomicrofluidics* **10** 024114

[12] Chen J, Zheng Y, Tan Q, Zhang Y L, Li J and Geddie W R *et al* 2011 A microfluidic device for simultaneous electrical and mechanical measurements on single cells *Biomicrofluidics* **5** 014113

[13] Ahrberg C D, Manz A and Chung B G 2016 Polymerase chain reaction in microfluidic devices *Lab Chip.* **16** 3866–84
[14] Chan K, Wong P-Y, Yu P, Hardick J, Wong K-Y and Wilson S A *et al* 2016 A rapid and low-cost PCR thermal cycler for infectious disease diagnostics *PLoS One* **11** e0149150
[15] Sugumar D, Ismail A, Ravichandran M, Aziah I and Kong L X 2010 Amplification of SPPS150 and *Salmonella typhi* DNA with a high throughput oscillating flow polymerase chain reaction device *Biomicrofluidics* **4** 024103
[16] Moschou D, Vourdas N, Kokkoris G, Papadakis G, Parthenios J and Chatzandroulis S *et al* 2014 All-plastic, low-power, disposable, continuous-flow PCR chip with integrated micro-heaters for rapid DNA amplification *Sens. Actuators* B **199** 470–8
[17] Zhu Y, Zhang Y-X, Liu W-W, Ma Y, Fang Q and Yao B 2015 Printing 2-dimentional droplet array for single-cell reverse transcription quantitative PCR assay with a microfluidic robot *Sci. Rep.* **5** 9551
[18] Floren C, Wiedemann I, Brenig B, Schütz E and Beck J 2015 Species identification and quantification in meat and meat products using droplet digital PCR (ddPCR) *Food Chem.* **173** 1054–8
[19] Hoshino T and Inagaki F 2012 Molecular quantification of environmental DNA using microfluidics and digital PCR *Syst. Appl. Microbiol.* **35** 390–5
[20] Gu S, Lu Y, Ding Y, Li L, Song H and Wang J *et al* 2014 A droplet-based microfluidic electrochemical sensor using platinum-black microelectrode and its application in high sensitive glucose sensing *Biosens. Bioelectron* **55** 106–12
[21] Lee K-H, Su Y-D, Chen S-J, Tseng F-G and Lee G-B 2007 Microfluidic systems integrated with two-dimensional surface plasmon resonance phase imaging systems for microarray immunoassay *Biosens. Bioelectron* **23** 466–72
[22] Matharu Z, Patel D, Gao Y, Haque A, Zhou Q and Revzin A 2014 Detecting transforming growth factor-β release from liver cells using an aptasensor integrated with microfluidics *Anal. Chem.* **86** 8865–72
[23] Bhatia S N and Ingber D E 2014 Microfluidic organs-on-chips *Nat. Biotechnol.* **32** 760–72
[24] Huh D, Matthews B D, Mammoto A, Montoya-Zavala M, Hsin H Y and Ingber D E 2010 Reconstituting organ-level lung functions on a chip *Science* **328** 1662–8
[25] Fan Y, Nguyen D T, Akay Y, Xu F and Akay M 2016 Engineering a brain cancer chip for high-throughput drug screening *Sci. Rep.* **6** 25062
[26] Theobald J, Ghanem A, Wallisch P, Banaeiyan A A, Andrade-Navarro M A and Taškova K *et al* 2018 Liver-kidney-on-chip to study toxicity of drug metabolites *ACS Biomater. Sci. Eng.* **4** 78–89
[27] Agarwal A, Goss J A, Cho A, McCain M L and Parker K K 2013 Microfluidic heart on a chip for higher throughput pharmacological studies *Lab Chip.* **13** 3599–608
[28] Kim S, Kim W, Lim S and Jeon J S 2017 Vasculature-on-a-chip for *in vitro* disease models *Bioengineering* **4** 8
[29] Sleeboom J J, Amirabadi H E, Nair P, Sahlgren C M and Den Toonder J M 2018 Metastasis in context: modeling the tumor microenvironment with cancer-on-a-chip approaches *Dis. Model Mech.* **11** dmm033100